Fermilab

Interplay between time and energy in bosonic noisy quantum metrology

FERMILAB-PUB-24-0894-SQMS-V

arXiv:2409.18791

Interplay between time and energy in bosonic noisy quantum metrology

Wojciech Górecki,[1] Francesco Albarelli,[2] Simone Felicetti,[3,4] Roberto Di Candia,[5,6] and Lorenzo Maccone[1,6]

[1]*INFN Sez. Pavia, via Bassi 6, I-27100 Pavia, Italy*
[2]*Scuola Normale Superiore, I-56126 Pisa, Italy*
[3]*Institute for Complex Systems, National Research Council (ISC-CNR), Via dei Taurini 19, 00185 Rome, Italy*
[4]*Physics Department, Sapienza University, P.le A. Moro 2, 00185 Rome, Italy*
[5]*Department of Information and Communications Engineering, Aalto University, Espoo, 02150 Finland*
[6]*Dip. Fisica, University of Pavia, via Bassi 6, I-27100 Pavia, Italy*

When using infinite-dimensional probes (such as a bosonic mode), one could in principle obtain infinite precision when estimating some physical parameters. This is unphysical, as it would require infinite resources, so one needs to impose some additional constraint: typically the average energy employed by the probe is finite. Here we treat both energy and time as a resource, showing that, in the presence of noise, there is a nontrivial interplay between the average energy and the time devoted to the estimation. Our results are valid for the most general metrological schemes (e.g. adaptive schemes which may involve entanglement with external ancillae). We apply recently derived precision bounds for all parameters characterizing the paradigmatic case of a bosonic mode, subject to Linbladian noise. We show how the time employed in the estimation should be partitioned in order to achieve the best possible precision. In most cases, the optimal performance may be obtained without the necessity of adaptivity or entanglement with ancilla. We compare results with optimal classical strategies. Interestingly, for temperature estimation, applying a fast-prepare-and-measure protocol with Fock states provides better scaling with the number of photons than any classical strategy.

I. INTRODUCTION

The use of nonclassical properties in quantum metrology, such as entanglement and squeezing, makes it possible to overcome the shot noise limit and achieve a quadratic scaling of measurement precision with the amount of resources, known as Heisenberg scaling [1–9]. Typically, in the presence of noise, Heisenberg scaling is not possible for a large number of resources, and the quantum advantage comes down to a constant, whose exact value depends on the intensity of the noise [10–16].

Often, one does not consider time as a resource in the estimation, but this has to be considered when analyzing practical scenarios: it is quite obvious that, in general, by devoting more time to measurement, one can obtain an increase in precision. In most papers about fundamental bounds including time, only small systems of non-scalable size are discussed [17, 18], while the dependence of both time and energy/size appears only in [19, 20], where the general framework is provided. Here we consider explicit case studies to show how time must be considered as a resource, emphasizing the comparison between optimal classical and quantum strategies. In general, it is not a priori clear how the available time should be allocated to get the optimal possible precision. For example, consider the simple noiseless situation where one wants to estimate a parameter φ using a unitary transformation $\exp(-it\varphi G)$ that acts on some probe state. Then, the quantum Cramér-Rao bound (when applicable) gives $\Delta^2\varphi \geqslant 1/(4t^2\Delta^2 G) \gtrsim 1/t^2N^2$, in terms of the average "energy" N and the time t, where $\Delta^2\varphi$ is the variance of any (unbiased) estimator, $\Delta^2 G$ is the variance of the generator G and we consider situations where $\Delta G \lesssim N$ (the opposite regime is useless for estimation [21]). For generic noise models, typically the Heisenberg scaling is lost for both time and energy, leading to standard scaling $\sim 1/tN$ [19, 20]. Optimization of the protocol requires consideration of the fact that often highly entangled states are more sensitive to noise, so one may take advantage of them only in a very short evolution. As a result, a compromise must be found between taking more advantage from entanglement or from a longer time of evolution.

Parameter	Coherent light	Quantum bound	Sec.
Frequency ω	$0.37 \times \frac{4N}{\Gamma(1+2n_B)}$	$\frac{4N}{\Gamma(1+2n_B)}$	III A
Displacement α	$0.82 \times \frac{4}{\Gamma}$	$\frac{4}{\Gamma}$	III B
Squeezing ϵ	–	$\frac{4(2N+1)}{\Gamma\sqrt{n_E(1+n_E)}}$	III C
Loss rate Γ	$0.37 \times \frac{N}{\Gamma(1+2n_E)}$	$\frac{N(1+2n_E)}{\Gamma}$	IV A
Temperature n_E	$\frac{\Gamma}{n_E}$	$N \times \frac{\Gamma(1+2n_E)}{n_E(1+n_E)}$	IV B

FIG. 1. Summary of the results. Optimal signal-to-noise ratio per time $S(t)/t$ for estimation of five different parameters. We consider a single-mode bosonic system coupled to a thermal bath. N is the mean number of photons, Γ is the constant of coupling with the thermal bath (loss rate) and n_E is the mean number of thermal photons. For simplicity of formulas, limits of large N are taken. In the column "coherent light" we present the results obtainable by classical strategy, i.e. optimal usage of the classical (coherent) state of light. In the column "quantum bound" we present a fundamental bound, that cannot be beaten by any quantum strategy (even the one including adaptiveness); in the main text, we present exemplary strategies saturating these bounds. One can see that in the temperature estimation using quantum strategy allows for the advantage scalable with the number of photons. For squeezing estimation, there is no "classical" counterpart, as the Hamiltonian itself creates squeezing.

In this work we provide a systematic analysis of parameter estimation for a paradigmatic, experimentally relevant model: a single bosonic mode connected to a thermal bath.

We consider both Hamiltonian estimation (frequency, displacement, squeezing) and noise-parameter estimation (loss rate, temperature), all in the finite temperature regime. We derive the fundamental bounds for these cases using the results in [19, 20], valid even for arbitrary strategies. These include the use of ancillary degrees of freedom and adaptivity, e.g. continuous measurement and feedback [22–25], and exploiting quantum criticality [26–33], as well as combining both approaches [34–36]. Furthermore, we propose practical protocols that saturate the optimal bounds. For most parameters, these optimal protocols only require feasible operations, readily available in relevant quantum platforms such as superconducting circuits, trapped ions, opto- and electro-mechanical systems, among others.

We show that for frequency and displacement estimation, almost optimal performance may be already obtained by using classical states of light if the total time is sufficiently large. Nonclassical light still may be useful in the case of the limited time of evolution. On the contrary, noise estimation involving a nonclassical input state allows for better scaling of the precision with temperature (for loss rate) or with a number of photons in the cavity (for temperature estimation); here optimal performance may be obtained by the fast-prepare-and-measure protocol. For squeezing estimation, there is no classical counterpart. Importantly, the bound increases infinitely in the limit of temperature going to 0. In this limit, we propose a protocol based on error correction that achieves a variance $\propto 1/tN^2$. The results are summarized in Fig. 1.

II. GENERAL FRAMEWORK

In this section we introduce the general framework and tools for noisy parameter estimation [19, 20]. While in the main part of the paper we will apply them to the single-mode bosonic model, here we keep the presentation more general and abstract, to stress the fact, that they can be directly used also to analyze other models.

A. Problem formulation

Consider a general Lindblad evolution:

$$\frac{d\rho}{dt} = -i[H,\rho] + \sum_{j=1}^{J} L_j \rho L_j^\dagger - \frac{1}{2}\rho L_j^\dagger L_j - \frac{1}{2} L_j^\dagger L_j \rho, \quad (1)$$

where H and L_j are the operators acting on the system $\mathcal{H}_S$ which may depend on the unknown parameter φ to estimate. Let us consider the most general metrological protocol. I.e., we assume that the system may be entangled with a noiseless ancilla $\mathcal{H}_A$ of arbitrary dimension (so that the Hamiltonian and Lindblad operators act on the joint Hilbert space as $H \otimes \mathbb{1}_A$ and $L_j \otimes \mathbb{1}_A$ respectively); moreover, we allow for an additional unitary $V(t)$ (acting jointly on $\mathcal{H}_S \otimes \mathcal{H}_A$) which is fully flexible, and controlled by experimentalists. Finally, the observable $\hat{O}$ is measured on the joint output state. We look at the quantum Fisher information (QFI) of the output state, which is equal to the signal-to-noise ratio (SNR) optimized over the possible choices of the measured observable:

$$I_\varphi = \max_{\hat{O}} S, \quad \text{where} \quad S = \frac{|\partial_\varphi \langle \hat{O} \rangle|^2}{\Delta^2 \hat{O}}. \quad (2)$$

(From the point of view of the local estimation, optimization over a single observable is equivalent to joint optimization over measurement and estimator, see App. A for formal derivation). We assume an ideal scenario, where both state preparation and the measurement procedure may be done immediately, so only sensing takes time. Therefore, any bound derived for such an ideal scenario will still be valid for any more realistic situation.

If quadratic scaling with an arbitrarily long time is obtainable, then the optimal strategy is to use all available time coherently in a single realization in the experiment. However, in the occurrence of noise, for typical protocols, QFI grows only up to a certain point. Therefore, at some point, it is better to interrupt the measurement and re-start the procedure from the beginning. The QFI scales linearly with the number of repetitions. Having at our disposal total time T and spending time t for a single iteration, in principle, we are able to perform T/t repetitions, so the total QFI will be equal to $(T/t)\cdot I_\varphi(t)$. Therefore, to validate the usefulness of the given protocol (properly taking into account time as a resource) one should compare $\max_t I_\varphi(t)/t$.

B. Noisy bounds

Let us start with an estimation problem, where the parameter dependence is in the Hamiltonian and denote derivative over this parameter by $\dot{H} := \partial_\varphi H$. In the absence of noise, the QFI is bounded by [28]:

$$I_\varphi(t) \leq 4 \left[\int_0^t \sqrt{\Delta^2 \dot{H}}\, dt' \right]^2. \quad (3)$$

Especially, for the simple case $H = \varphi G$, we recover the standard formula $I_\varphi(t) \leq 4t^2 \Delta^2 G$.

While this bound is derived for noiseless Hamiltonian dynamics, it applies also in the presence of noise. In this case, it can typically be saturated for sufficiently small times, when the evolution is almost unitary.

However, for most generic noise quadratic scaling with time occurs only at the beginning, while later it becomes linear. More formally, quadratic scaling for large times is possible if and only if the generator of the evolution cannot be expressed as a quadratic combination of Lindblad operators

$$\dot{H} \notin \text{span}_{\mathbb{C}}\{\mathbb{1}, L_i, L_i^\dagger, L_i^\dagger L_j\}. \quad (4)$$

This is the so-called Hamiltonian-not-in-Lindblad-Space (HNLS) condition [17]. Otherwise, QFI is bounded by

[19, 20]:

$$I_\varphi(t) \leq 4\int_0^t \langle \mathfrak{a}(h)\rangle_{t'}\, dt', \quad \text{with} \quad \mathfrak{b}(h)=0, \tag{5}$$

where $\langle\cdot\rangle_{t'} := \mathrm{Tr}(\rho(t')\cdot)$, and $\mathfrak{a}(h)$ and $\mathfrak{b}(h)$ are the following operators acting on the system:

$$\mathfrak{a}(h) = \left(\mathfrak{h}\vec{L}+\vec{h}\mathbb{1}\right)^\dagger \cdot \left(\mathfrak{h}\vec{L}+\vec{h}\mathbb{1}\right), \tag{6}$$

$$\mathfrak{b}(h) = \dot{H} + h_{00}\mathbb{1} + \vec{h}^\dagger\cdot\vec{L} + \vec{L}^\dagger\cdot\vec{h} + \vec{L}^\dagger\cdot\mathfrak{h}\cdot\vec{L}. \tag{7}$$

Here $\vec{L}$ is a vector of Lindblad operators, while the free parameters: real scalar $h_{00}\in\mathbb{R}$, complex vector $\vec{h}\in\mathbb{C}^J$, and hermitian matrix $\mathfrak{h}\in\mathbb{C}_{\mathrm{H}}^{J\times J}$, are jointly denoted by the letter h. The bound is valid for any h satisfying $\mathfrak{b}(h)=0$ and may be tightened by optimization over h.

The time dependence of $\Delta^2 \dot{H}$ and $\langle\mathfrak{a}(h)\rangle_{t'}$ may be essential in analyzing critical metrology, where the average values of observables and their variances are changing significantly during evolution. For the passive strategies (no additional action is performed during the evolution time, and a measurement is performed after), they do not change their order of magnitude and comparing the bounds Eq. (3) and Eq. (5) gives the characteristic time for which the scaling goes from quadratic to linear $\tau \sim \langle\mathfrak{a}(h)\rangle/\Delta^2\dot{H}$ [18]. In the intermediate regime, slightly tighter bounds may be derived [20], see App. B for details.

If the total available time is much longer than τ, then, according to the discussion from the previous section, in validating the measurement protocol it is reasonable to look at the ratio $I_\varphi(t)/t$. For simplicity of further formulas, we may also bound the integral in Eq. (5) by the maximal value of the function under the integral to obtain:

$$\frac{I_\varphi(t)}{t} \leq 4\langle\mathfrak{a}(h)\rangle_{\max}, \quad \text{with} \quad \mathfrak{b}(h)=0, \tag{8}$$

where $\langle\mathfrak{a}(h)\rangle_{\max} := \max_{t'\in[0,t]}\langle\mathfrak{a}(h)\rangle_{t'}$. This inequality will be the main point of reference in discussing examples.

III. HAMILTONIAN PARAMETER ESTIMATION

We analyze several specific estimation strategies for a single-mode system coupled to a thermal bath:

$$\frac{d\rho}{dt} = -i[H,\rho] + \Gamma(1+n_E)\left(a\rho a^\dagger - \frac{1}{2}\{a^\dagger a,\rho\}\right) + \Gamma n_E\left(a^\dagger\rho a - \frac{1}{2}\{aa^\dagger,\rho\}\right), \tag{9}$$

so the Lindblad operators are $L_1=\sqrt{\Gamma(1+n_E)}a$ and $L_2=\sqrt{\Gamma n_E}a^\dagger$.

A. Frequency estimation

We start with the problem of frequency estimation, i.e. the Hamiltonian is given as:

$$H = \omega a^\dagger a, \tag{10}$$

and ω is the parameter to be estimated. The bound Eq. (8) reads (see App. C for derivation):

$$\frac{I_\omega(t)}{t} \leq \frac{4\langle a^\dagger a\rangle_{\max}}{\Gamma(1+2n_E-\frac{n_E}{\langle a^\dagger a\rangle_{\max}+1})} \approx \frac{4\langle a^\dagger a\rangle_{\max}}{\Gamma(1+2n_E)}, \tag{11}$$

so it scales linearly with the number of photons. Note, that the bound on the mean number of photons solely does not impose any bound on its variance, so without additional assumption we cannot say anything about the characteristic time of transition τ. However, restricting to Gaussian states we have $\Delta^2 N \leq 2N(N+1)$, and then:

$$\tau \gtrsim \frac{1}{2(N+1)\Gamma(1+2n_E)}. \tag{12}$$

To understand it better, consider an input state to be a vacuum squeezed along the x axis, shifted along the p axis $\mathcal{D}(i\alpha)S(r)|0\rangle$, where $\mathcal{D}$ and S are the displacement and squeezing operators, so the initial number of photons is $N=\alpha^2+\sinh^2 r$, with $\alpha\in\mathbb{R}$. Without loss of generality, we may assume that we work around the point $\omega\approx 0$ (otherwise we rotate the frame of reference). After rotating for a time t, one performs homodyne detection in direction $\hat{x}=a+a^\dagger$. As:

$$\begin{aligned}\langle\hat{x}(t)\rangle &= 2\alpha e^{-\Gamma t/2}\sin(\omega t)\\ \Delta^2\hat{x}(t) &= e^{-\Gamma t}e^{-2r} + (1-e^{-\Gamma t})(1+2n_E),\end{aligned} \tag{13}$$

The SNR is equal to

$$S(\omega) = \frac{4\alpha^2 t^2}{e^{-2r}+(e^{\Gamma t}-1)(1+2n_E)}. \tag{14}$$

It gives a very simple interpretation of the scaling with both t and N, which has a different origin.

For small times (compared to the loss rate), the signal is coherently accumulated over time, resulting in t^2 scaling of SNR. In the case of photons, the light intensity α^2 multiplies signal strength, while squeezing factor e^{-2r} is responsible for reducing noise. Especially, in the unitary case $\Gamma=0$, for obtaining quadratic scaling with time it is enough to evolve state freely. Obtaining quadratic scaling with N required an equal distribution of achievable photons between α^2 and $\sinh^2 r$.

For $\Gamma>0$, if the time t is strictly limited, obtaining the optimal scaling with the system parameters requires using a nonclassical input state. That may be the case in the situation, where the signal appears only for some limited time, of order $1/\Gamma$ or smaller. The optimal rate of squeezing then depends on the exact values of t, N, Γ. In the limit of large N, for $1/N \ll e^{-2r} \ll \Gamma t \ll 1$, approximately the whole energy is put into the displacement $N\approx\alpha^2$, and Eq. (14) divided by time converge to Eq. (11).

Note, however, that if the total time $t \gg 1/\Gamma$ and one has the freedom to divide it into optimal slots, very similar results may be obtained by using a coherent state (so $r=0$) and letting it evolve by time $1/\Gamma$ in each iteration. Then one loses at most $1/e$ factor compared to the bound, similar to [37], while for finite temperature $n_E>0$ the loss is even smaller.

Indeed, using a squeezed state significantly reduces the variance of measurement results, but this effect disappears

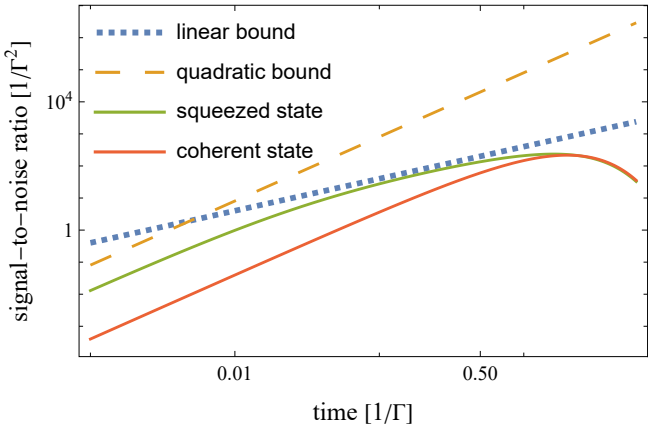

FIG. 2. Relation between exemplary metrological strategies and fundamental bounds for precision on the example of frequency estimation. Both quadratic one Eq. (3) and linear one Eq. (5) are valid during the whole time of the evolution, for any strategy of given average energy. The quadratic one is tighter for $t \ll 1/\Gamma$ and the linear one is tighter for $t \gtrsim 1/\Gamma$. Comparing specific strategies, we see that for small times the squeezed state performs significantly better than the coherent one. However, it also transfers from quadratic to linear scaling faster. At the optimal time, they perform similarly, both close to the bound.

sharply for times longer than e^{-2r}/Γ. Contrary, the optimal signal accumulation requires times of order $1/\Gamma$. As a consequence, one must choose if one wants to take more benefits from entanglement between photons or from coherence in time, but one cannot use both of them simultaneously, see Fig. 2.

The bound ensures us that this problem cannot be overcome even with more advanced methods and applying additional entanglement with an ancilla and/or action during evolution. Especially, in [31] the additional squeezing term $+\epsilon(a^{\dagger 2} + a^2)$ has been added to Eq. (9), which results in critical behavior around the point $\epsilon = \sqrt{\omega^2 + \Gamma^2}$. As shown, it allows for arbitrary lengthening of quadratic scaling time, while simultaneously reducing the scaling constant and effectively leading to an analogous result.

Note that here we assume that n_E is a constant independent on ω. This is a common and good approximation, as typically the knowledge about ω which could be taken from measuring n_E is negligible. Yet, one should remember, that in reality, a more reasonable assumption is $n_E = 1/(e^{\hbar\omega/k_B T} - 1)$, which becomes relevant if the measurement is performed on a steady state [38].

B. Displacement estimation

Now let us discuss displacement estimation, i.e.

$$H = i\alpha(a^\dagger - a), \tag{15}$$

where we assume, that displacement direction is known, so that the parameter to be estimated is just the real coefficient α. The bound Eq. (8) reads (App. C):

$$\frac{I_\alpha(t)}{t} \leq \frac{4}{\Gamma(1 + 2n_E)}. \tag{16}$$

Unlike in the previous example, here the constraint on a mean number of photons implies the bound on $\Delta^2\dot{H}$, $\Delta^2\dot{H} \leq 4N + 2$, so:

$$\tau \gtrsim \frac{1}{(4N + 2)\Gamma(1 + 2n_E)}. \tag{17}$$

We see that the bound for precision Eq. (16) does not scale with N at all, unlike in the previously discussed case. It may be easily understood, as in this model there is no point in using displacement while preparing the state (as it commutes with the Hamiltonian), while squeezing, similarly as in the previous case, may only lead to a constant advantage. Indeed, for squeezed vacuum as input:

$$\begin{aligned} \langle \hat{x}(t) \rangle &= 2\alpha(1 - e^{-t\Gamma/2})/(\Gamma/2), \\ \Delta^2 \hat{x}(t) &= e^{-\Gamma t} e^{-2r} + (1 - e^{-\Gamma t})(1 + 2n_E), \end{aligned} \tag{18}$$

so the SNR per time is:

$$\frac{S_\alpha(t)}{t} = \frac{16(1 - e^{t\Gamma/2})^2}{\Gamma^2(e^{-\Gamma t} e^{-2r} + (1 - e^{-\Gamma t})(1 + 2n_E))t}. \tag{19}$$

Again, the bound may be asymptotically saturated if $e^{-2r} \ll \Gamma t \ll 1$. Similarly, as in the previous case, almost optimal results may be also obtained without squeezing, by choosing the optimal time of a single iteration, leading finally to a factor ~ 3.26 instead of 4 in the nominator.

C. Squeezing estimation

In this section, we consider the estimation of the squeezing parameter (see also [39]). Consider a system coupled with the thermal bath Eq. (9) with the Hamiltonian:

$$H = \epsilon(a^2 + a^{\dagger 2}), \tag{20}$$

where the parameter ϵ is to be measured. The bound Eq. (8) reads:

$$\frac{I_\epsilon(t)}{t} \leq \frac{4(2N + 1)}{\Gamma\sqrt{n_E(1 + n_E)}}. \tag{21}$$

Note that the bound goes to infinity as $n_E \to 0$. Indeed, if the bath is at zero temperature $n_E = 0$, we have only a single Lindblad operator $L = \sqrt{\Gamma}a$ and the condition $\mathfrak{b}(h) = 0$ cannot be satisfied for any choice of h, so in principle, the quadratic scaling with both number of photons and total time $I_\epsilon \sim N^2 t^2$ should be possible, even for arbitrarily long times.

From the theoretical point of view such scaling indeed may be obtained by applying a proper quantum error correction protocol [17], see App. D for details. In practice, its implementation for this model would pose many difficulties, mainly

due to the need for frequent projections onto non-trivial subspaces of Hilbert space. Moreover, for Heisenberg scaling with all resources, another issue arises, related to the fact that saturating the Cramér-Rao bound demands arbitrarily large prior [40–42].

Instead, we discuss here in detail a simpler protocol, leading to linear scaling with time, but providing quadratic scaling with the average number of photons in the system $I_\epsilon \sim N^2 t$ (in contrast to the examples discussed earlier, where such scaling was fundamentally forbidden).

The idea of this protocol is based on the observation that the evolution of the state coupled to a thermal bath may be seen as the deterministic decay followed by random quantum jump [43]. It allows for using code space based on cat states [44, 45]. Below we follow the notation from [45]. Consider cat states of the form:

$$\begin{aligned} |\mathcal{C}^{\pm}_{\alpha}\rangle &= \mathcal{N}(|\alpha\rangle \pm |-\alpha\rangle), \\ |\mathcal{C}^{\pm}_{i\alpha}\rangle &= \mathcal{N}(|i\alpha\rangle \pm |-i\alpha\rangle). \end{aligned} \tag{22}$$

For large α, all the states $|\alpha\rangle$, $|-\alpha\rangle$, $|i\alpha\rangle$ and $|-i\alpha\rangle$ are almost orthogonal and the normalization constant $\mathcal{N} \approx \frac{1}{\sqrt{2}}$. A logical qubit may be encoded in $|\psi^{(0)}_\alpha\rangle = c_g |\mathcal{C}^+_\alpha\rangle + c_e |\mathcal{C}^+_{i\alpha}\rangle$. Note that the action of subsequent quantum jumps results with:

$$\begin{aligned} |\psi^{(0)}_\alpha\rangle &:= c_g |\mathcal{C}^+_\alpha\rangle + c_e |\mathcal{C}^+_{i\alpha}\rangle , \\ a\,|\psi^{(0)}_\alpha\rangle \propto |\psi^{(1)}_\alpha\rangle &:= c_g |\mathcal{C}^-_\alpha\rangle + i c_e |\mathcal{C}^-_{i\alpha}\rangle , \\ a^2\,|\psi^{(0)}_\alpha\rangle \propto |\psi^{(2)}_\alpha\rangle &:= c_g |\mathcal{C}^+_\alpha\rangle - c_e |\mathcal{C}^+_{i\alpha}\rangle , \\ a^3\,|\psi^{(0)}_\alpha\rangle \propto |\psi^{(3)}_\alpha\rangle &:= c_g |\mathcal{C}^-_\alpha\rangle - i c_e |\mathcal{C}^-_{i\alpha}\rangle . \end{aligned} \tag{23}$$

Importantly, each of them has well-defined photon parity, which is changed after each quantum jump. Therefore, by applying non-demolition parity measurement [45], one may efficiently keep the knowledge about actual states, without affecting the relative quantum phase. Moreover, due to deterministic decay, for all states $\alpha \to e^{-\Gamma t/2}\alpha$ in time.

Let us now look at how useful this protocol can be for squeezing estimation. Let us define a proper even (+) and odd (-) code spaces as $H_{\mathcal{C}^\pm} := \mathrm{span}\{|\mathcal{C}^\pm_\alpha\rangle, |\mathcal{C}^\pm_{i\alpha}\rangle\}$. The Hamiltonian acts non-trivially inside of both these code spaces:

$$\begin{aligned} H_{\mathcal{C}^\pm} &:= \Pi_{\mathcal{C}^\pm} \epsilon (a^{\dagger 2} + a^2) \Pi_{\mathcal{C}^\pm} \\ &= 2\epsilon \mathrm{Re}(\alpha^2) \left(|\mathcal{C}^\pm_\alpha\rangle\langle\mathcal{C}^\pm_\alpha| - |\mathcal{C}^\pm_{i\alpha}\rangle\langle\mathcal{C}^\pm_{i\alpha}| \right). \end{aligned} \tag{24}$$

Therefore, the evolution of the state $|\psi^{(0)}_\alpha\rangle = \frac{1}{\sqrt{2}}(|\mathcal{C}^+_\alpha\rangle + |\mathcal{C}^+_{i\alpha}\rangle)$ will be sensitive to changes of ϵ. As we noted, the noise does not take us outside of these two subspaces.

The only potential problem is that the acting of the measured Hamiltonian may create a leakage outside of them. Neverless, as for large $|\alpha|^2$ in the leading therm $a^\dagger |\alpha\rangle$ may be approximated by $\alpha^* |\alpha\rangle$, the amount of leakage will remain negligible for $t\epsilon \ll 1/\sqrt{N+2}$, see App. E for details. Note especially, that this condition may be satisfied even for large N, if one has approximated knowledge about the value of the squeezing parameter. Then one can apply anti-squeezing as well, to keep the effective squeezing parameter measured around 0.

Assuming that the above condition is satisfied (i.e. the effect of leakage may be neglected), the evolution of the states will be given as:

$$|\psi(t)\rangle = \frac{1}{\sqrt{2}} \left[e^{-i\varphi(t)} |\mathcal{C}^{(-1)^n}_{\alpha e^{-t\Gamma/2}}\rangle + e^{i\varphi(t)} i^n |\mathcal{C}^{(-1)^n}_{i\alpha e^{-t\Gamma/2}}\rangle \right], \tag{25}$$

where n is the number of jumps and $\varphi(t)$ is the phase accumulated during evolution:

$$\varphi(t) = \int_0^t 2\epsilon \mathrm{Re}(\alpha(t')^2) dt' = 2\epsilon\alpha^2(1 - e^{-t\Gamma})/\Gamma. \tag{26}$$

As the number of jumps n is monitored, one effectively deals with a single qubit. Therefore $I_\epsilon(t) = 16N^2(1-e^{-t\Gamma})^2/\Gamma^2$, so

$$\max_t \frac{I_\epsilon(t)}{t} = 6.56 \times \frac{N^2}{\Gamma}, \tag{27}$$

which is obtained for $t = 1.26/\Gamma$.

IV. NOISE ESTIMATION

The second class of estimation protocols we discuss is noise estimation. I.e., we assume that the parameter is encoded solely in the dissipative part of the Lindblad equation Eq. (9). Moreover, we assume, that the parameter does not change the "type" of noise, but only its magnitude. I.e., the parameter is encoded in the scalars multiplying Lindblad operators. Then QFI arises at most linearly with time and it is bounded by [20]:

$$\frac{I_\varphi(t)}{t} \leq \langle \dot{\vec{L}}^\dagger \dot{\vec{L}} \rangle_{\max}. \tag{28}$$

That will be the case in the problem of the temperature of thermal bath estimation and the loss rate estimation. For the more general cases, where the change in parameter changes the shape of Lindblad operators, see App. B. In contrast to unitary evolution, when for small times QFI arises quadratically, so the minimal time of a single iteration is required for optimal performance, in the noise estimation, this time may be arbitrarily short. We only need to remember that the Lindblad equation itself comes from averaging over some finite time so that the analysis for the smaller time scales is trivially nonmeaningful (as it would require a microscopic description that goes beyond the approximations implicit in the Master equation).

In the examples discussed so far, the parameter value was estimated from the mean value of the measured observable, so the variance of the estimator could be calculated from the error propagation formula (the inverse of the SNR). In general, by having access to the full statistics of the measurement results, better precision can sometimes be achieved by choosing a more efficient estimator. Let $p_\varphi(i)$ be the probability of obtaining the measurement result i, while the true value of the parameter is φ. Then classical Fisher information (FI) is given as:

$$F_\varphi = \sum_i \frac{1}{p_\varphi(i)} \left(\frac{\partial p_\varphi(i)}{\partial \varphi} \right)^2. \tag{29}$$

Consider fixed positive operator-valued measure (POVM) $\{M_i\}_i$, so $p_\varphi(i) = \mathrm{Tr}(\rho_\varphi M_i)$. Then we may define observable as $\hat{O} = \sum_i \tilde{\varphi}(i) M_i$ and FI may be seen as the SNR Eq. (2) optimized over $\tilde{\varphi}(i)$ with fixed M_i.

A. Loss rate estimation

We consider again the system governed by the equation Eq. (9) with $H = 0$, where the parameter to be estimated is Γ. The bound Eq. (28) gives:

$$\frac{I_\Gamma(t)}{t} \leq \frac{\langle a^\dagger a\rangle_{\max}(1+2n_E)}{\Gamma} + \frac{n_E}{\Gamma}. \tag{30}$$

For the squeezed displaced state of light $\mathcal{D}(\alpha)S(r)\left|0\right\rangle$ as an input (in this case squeezing is in the same direction as displacement), we have:

$$\begin{aligned} \langle \hat{x}(t)\rangle &= 2\alpha e^{-\Gamma t/2} \\ \Delta^2\hat{x}(t) &= e^{-2r}e^{-\Gamma t} + (1-e^{-\Gamma t})(1+2n_E), \end{aligned} \tag{31}$$

so

$$\frac{S_\Gamma(t)}{t} = \frac{\alpha^2 t}{e^{-2r} + (e^{\Gamma t}-1)(1+2n_E)}. \tag{32}$$

Note, that the formula for the SNR is exactly the same as the one for frequency estimation. Indeed, while looking only at averages of quadratures, in both cases small changes of the parameter result in the displacement being multiplied by α^2. Therefore, similar as in frequency estimation, for $1/N \ll e^{-2r} \ll \Gamma t \ll 1$ we obtain roughly $S_\Gamma(t)/t \approx N/\Gamma(1+2n_E)$, while for using coherent light for time $t = 1/\Gamma$ we loose only a constant factor of order $1/e$. See also [46, 47] for more relations between frequency and loss estimation.

While in the limit of small temperature $n_E \to 0$ these results are close to saturating the bound of Eq. (30), they completely fail for large temperature (where, looking at the bound, in principle a larger temperature may help). One may notice that, unlike ω in frequency estimation, the changes of parameter Γ affect not only the mean of the Gaussian but its covariance matrix as well, so the homodyne detection is no longer the optimal measurement[1].

Indeed, to saturate the bound Eq. (30) let us consider a squeezed vacuum state, which is known to be a superposition of the Fock state with an even number of photons. For a short time, approximately only one photon will be lost or taken from the environment. As a result, the probability that after small time $tN\Gamma(1+n_E) \ll 1$ the photon number is odd is given by: $p_{\text{odd}} \approx \Gamma t\left[(1+2n_E)N + n_E\right]$, see App. F. Using the formula for classical FI we immediately see, that the parity measurement saturates Eq. (30). Note, that the parity measurement may be easily realized as a quantum nondemolition measurement (QND) [45], which makes this strategy especially useful in practice.

The problem has been analyzed before in non-adaptive scenarios in both zero temperature case [48, 49] and finite temperature case [50, 51], which converge to our results after taking proper limits. An alternative derivation of the bound appears in [52], leading to a looser bound. Contrary to all mentioned papers, our bound is guaranteed to remain valid for any adaptive strategy (see [53] for example, where non-linearity is added to Hamiltonian).

B. Temperature estimation n_E

Here we consider the estimation of temperature n_E. Note the difference with equilibrium thermometry, where the system is known to be in the Gibbs state. On the contrary, here we consider dynamical protocols, where unitary operations and measurements can be implemented before reaching equilibrium [54]. Only such an approach allows for properly including the total time as a resource. In such formulation, the problem has been intensively discussed for finite-dimensional systems in [55]. Effectively, the parameter to be estimated is n_E is included in scalars multiplying Lindblad operators.

For the estimation of the parameter n_E, the bound Eq. (28) gives:

$$\frac{I_{n_E}(t)}{t} \leq \frac{(1+2n_E)\langle a^\dagger a\rangle_{\max}\Gamma}{n_E(1+n_E)} + \frac{\Gamma}{n_E} \tag{33}$$

Similarly to the previous case, the bounds scale linearly with the number of photons. Note, however, that here using a coherent state offers no advantage over using a vacuum—indeed, the output state is the same as for the vacuum, only displaced by an n_E-independent factor. Therefore, for obtaining the optimal possible scaling with N it is necessary to use a nonclassical state of light.

As an exemplary strategy for saturating the bound consider preparing the initial state as the Fock state $\left|N\right\rangle$ and performing photon counting after a small time. For $tN\Gamma(1+n_E) \ll 1$, we have approximately (see App. G for exact formulas):

$$p(N) = 1 - tN\Gamma(1+n_E) - t(N+1)\Gamma n_E \tag{34}$$
$$p(N+1) = t(N+1)\Gamma n_E \tag{35}$$
$$p(N-1) = tN\Gamma(1+n_E). \tag{36}$$

The corresponding classical FI is equal:

$$F_{n_E} \overset{N t\Gamma \ll 1}{\approx} \frac{\Gamma N t(1+2n_E)}{n_E(1+n_E)} + \frac{\Gamma t}{n_E}, \tag{37}$$

so it saturates the bound. This strategy works similarly well for the previous problem of loss rate estimation Γ.

Note that, unlike in the case of loss estimation, the parity measurement would not be sufficient for optimal performance. This happens because for temperature estimation it is crucial to distinguish between the situation when a photon is lost and

[1] The only exception is a coherent state with zero-temperature bath. Then the covariance matrix is not affected by Γ and all information is included solely in the mean value of the position.

the one when it is taken from the environment. See App. F for the mathematical explanation.

A nondemolition photon counting measurement is more challenging to implement than a parity measurement. However, if one were able to perform it, it would be very useful for fast-prepare-and-measure protocols, as a post-measurement outcome would be a Fock state, which is ready for another iteration. See [56, 57] for current progress in the experimental application of similar strategy in analogous problems. A similar performance may be obtained by using a two-mode squeezed vacuum as an input state, while the second mode corresponds to noiseless ancilla [58].

For a better understanding, it is worth comparing this with the previously known bounds. The problem has been discussed in the literature, typically with the assumption that after preparing the state, it interacts freely with the bath for some fixed time t, after which a single measurement is performed.

In [50, 58] another bound based on channel purification has been derived, which for small t correspond with Eq. (33), see App. G for details. Another interesting bound is the one from [59], stating that:

$$I_{n_E}^{\text{single shot}} \leq \frac{1}{n_E(1+n_E)}, \tag{38}$$

and does not depend on t, N, Γ at all (while in practice the number of photon N needed for saturating this bound increases with inverse of $t\Gamma$). This can be intuitively understood because, for a very long time, the system fully thermalizes (while the time of thermalization depend on N, Γ).

More formally, the bound may be derived using the concept of quantum simulation [60, 61]. The free evolution of any input state of the cavity interacting with the bath may be equivalently obtained by mixing this state with a thermal state via beam-splitter with transmittance $\kappa = e^{-t\Gamma}$. As the beamsplitter itself does not depend on n_E, it is clear that the QFI of the final state of the system cannot be bigger than the QFI of the initial global state of both systems and environments, which is (due to the product structure of initial state) simply the QFI of the thermal state. This allows for bounding the problem of channel estimation by the simpler problem of state estimation.

Note, that the bound Eq. (38) does not contradict our results, but rather explains the origin of the advantage of using nonclassical states. Using more photons cannot overcome the bound Eq. (38), but it may allow for saturating it in a shorter time. As a consequence, using higher-energy Fock states more measurement repetitions may be performed in the same total time. Compared to previous results, our bound shows that this result cannot be overcome by using an adaptive strategy. The relation of our result to the existing bound is summarized in Fig. 3.

A comparison of Eq. (38) with Eq. (33) shows that, for optimal performance, the time of a single repetition cannot be longer than $t \sim 1/\Gamma N$. One should be careful with taking the limit $N \to \infty$, as then one can reach time scales so small, that the Lindblad equation is not valid any more.

Note, that the problem of temperature estimation is closely related to dark-matter sensing, where light displacement with a completely random direction is to be detected [58, 62], see App. H for details.

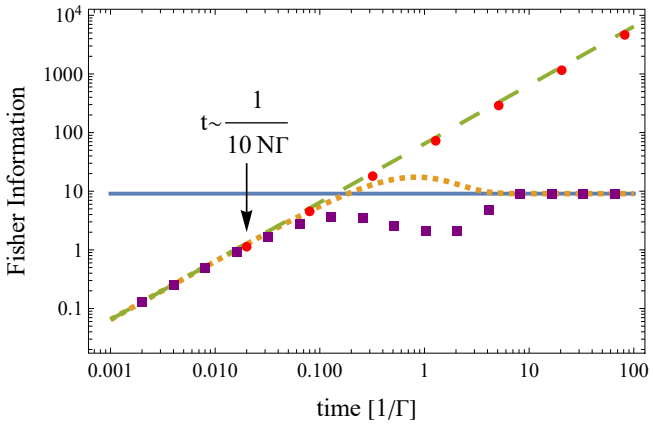

FIG. 3. The bounds for the Fisher information as the function of time and the result for some specific strategies. Calculations are made for $N = 5$ and $n_E = 0.1$. The blue solid line Eq. (38) and yellow dotted line Eq. (G2) correspond to the bounds from the literature, derived for passive strategies (no additional action is performed during time t and the measurement is performed after this time). Purple squares are the classical Fisher information for passive evolution of the Fock input state Eq. (G6). For a long time, the state became fully thermalized and FI converges to bound Eq. (38). Green dashed line Eq. (33) is a general bound for any strategy using total time t (including measurements between and/or any kind of adaptivity). Red dots represent an exemplary strategy saturating this bound, based on fast-prepare-and-measure protocol with Fock state with single-sensing time $t \sim 1/10N\Gamma$, without the necessity of any adaptivity.

Here the impact of temperature is modeled only via exchanging the photons with the environment. As pointed out in [55] (where the analysis has been performed for arbitrary finite-dimensional systems), it also causes a Lamb shift, which significantly affects the bound for QFI (especially for small temperatures), but its saturability is not clear.

V. CONCLUSIONS

We investigated the interplay between time and energy in quantum sensing with infinite-dimensional systems. We considered quantum estimation protocols for all the parameters of a minimal model for a quantum resonator in the open-quantum system setting. In particular, we considered noisy quantum estimation of frequency, squeezing, loss rate, and bath temperature. In all cases, we treat both the number of photons and sensing time as a resource. Comparing fundamental bounds with simple protocols, we found that for frequency and displacement estimation almost optimal performance may be obtained by using coherent light. On the contrary, in noise estimation optimal performance requires using of nonclassical states of light. Especially, in temperature estimation, it allows for a better scaling with the number of photons.

In the analysis, we did not include the system preparation time and measurement time, which we call jointly $t_{p,m}$. If one

were to include them, one should optimize $I(t)/(t+t_{p,m})$ instead of $I(t)/t$. However, regarding the analysis performed, the inclusion of these times would work in favor of the protocols with classical light over the ones with squeezed light (since for them the time of a single measurement is longer, so $I(t)/(t+t_{p,m})$ will suffer less from adding $t_{p,m}$. It is worth mentioning, that in this context the critical metrology may outperform both of them, as discussed in [31]. In the case of loss estimation, this problem may be completely omitted by using non-demolition parity measurement.

In this paper, we performed an analysis based on QFI and SNR. Even though this tool sometimes does not give the full picture when reaching the Heisenberg limit [8, 40–42, 63], in the cases discussed, the asymptotic scaling of precision with time was only linear, so the results obtained with these tools are fully trustable [64–67]. In addition, for example, the temperature estimation problem has also been discussed in the literature using Bayesian estimation theory (for the finite-dimensional case), with qualitatively similar results [68].

In conclusion, we have identified optimal strategies for noisy parameter estimation in a paradigmatic infinite-dimensional quantum model, of high experimental relevance. In doing so, we have also shown that fundamental bounds for arbitrary possible strategies, including adaptivity and ancillae, can be saturated by simple passive protocols in most cases. We believe these results show that deriving fundamental bounds for quantum metrology can have a concrete impact on the design of optimal protocols and practical sensing devices. In particular, we have also highlighted the usefulness of these bounds not only for Hamiltonian parameters but also for noise parameters. Since such methods are universal, we expect that they will be relevant in other scenarios and physical systems, including atoms or other quantum nonlinearities, e.g. to study the estimation of two-photon absorption [69–71].

ACKNOWLEDGEMENTS

This material is based upon work supported by the U.S. Department of Energy, Office of Science, National Quantum Information Science Research Centers, Superconducting Quantum Materials and Systems Center (SQMS) under the contract No. DE-AC02-07CH11359. F.A. acknowledges support from Marie Skłodowska-Curie Action EUHORIZON-MSCA-2021PF-01 (project QECANM, grant no. 101068347). S.F. acknowledges financial support from the foundation Compagnia di San Paolo, grant vEIcolo no. 121319, and from PNRR MUR project PE0000023-NQSTI financed by the European Union – Next Generation EU. R.D. acknowledges support from the Academy of Finland, grants no. 353832 and 349199. L.M. acknowledges support from the PNRR MUR Project PE0000023-NQSTI and from the National Research Centre for HPC, Big Data and Quantum Computing, PNRR MUR Project CN0000013-ICSC.

Appendix A: QFI as maximized SNR

Here we prove Eq. (2), i.e.:

$$I_\varphi = \max_{\hat{O}} S, \quad \text{where} \quad S = \frac{|\partial_\varphi \langle \hat{O} \rangle|^2}{\Delta^2 \hat{O}}. \tag{A1}$$

QFI by definition is equal to:

$$I_\varphi = \mathrm{Tr}(\rho_\varphi \Lambda^2), \tag{A2}$$

where symmetric logarithmic derivative Λ is a solution of:

$$\frac{1}{2}(\rho_\varphi \Lambda + \Lambda \rho_\varphi) = \frac{\partial \rho_\varphi}{\partial \varphi}. \tag{A3}$$

Now, let us look at the maximization of S over $\hat{O}$. As a formula for S is invariant for rescaling $\hat{O}$ by constant, without loss of generality we may impose condition $\mathrm{Tr}\left(\frac{\partial \rho_\varphi}{\partial \varphi}\hat{O}\right) = 1$. Then the problem reduces to minimization of $\Delta^2 \hat{O}$. Moreover, minimization of $\Delta^2 \hat{O}$ gives the same results as minimization of $\mathrm{Tr}(\rho_\varphi \hat{O}^2)$ (as one may always replace $\hat{O} \to \hat{O} - \mathrm{Tr}(\rho_\varphi \hat{O})\mathbb{1}$ without violating imposed condition). Therefore, the problem may be formulated as follows:

$$\min_{\hat{O}} \mathrm{Tr}(\rho_\varphi \hat{O}^2), \quad \text{with} \quad \mathrm{Tr}\left(\frac{\partial \rho_\varphi}{\partial \varphi}\hat{O}\right) = 1. \tag{A4}$$

To solve it, we use Lagrange's multipliers method. Consider small change $\hat{O} \to \hat{O} + \delta \hat{X}$, with δ being small scalar and $\hat{X}$ being arbitrary hermitian matrix. The solution needs to satisfy:

$$\mathrm{Tr}(\rho_\varphi (\hat{O}+\delta\hat{X})^2) = \lambda \mathrm{Tr}\left(\frac{\partial \rho_\varphi}{\partial \varphi}(\hat{O}+\delta\hat{X})\right) + \mathcal{O}(\delta^2), \tag{A5}$$

with λ being a Lagrange's multiplier. As it need to works for any $\hat{X}$, we have:

$$\rho_\varphi \hat{O} + \hat{O}\rho_\varphi = \lambda \frac{\partial \rho_\varphi}{\partial \varphi} \tag{A6}$$

One can see that the above equality is the same as Eq. (A3), up to a constant multiplicative factor λ, so $\hat{O}_{\text{opt}} = \frac{\lambda}{2}\Lambda$. Taking into account condition $\mathrm{Tr}\left(\frac{\partial \rho_\varphi}{\partial \varphi}\hat{O}_{\text{opt}}\right) = 1$, and using equality Eq. (A3) we find that $\lambda = \left[\mathrm{Tr}(\rho_\varphi \Lambda^2)\right]^{-1}$, so indeed:

$$\max_{\hat{O}} \frac{|\partial_\varphi \langle \hat{O} \rangle|^2}{\Delta^2 \hat{O}} = \mathrm{Tr}(\rho_\varphi \Lambda^2). \tag{A7}$$

Appendix B: General version of the bound

In the most general case, one may consider the situation when the parameter is encoded in both Hamiltonian and dissipative parts simultaneously. All bounds mentioned in the main text may be seen as the consequence of the bound for the derivative of QFI over time, being a generalization of the results from [16, 18] for unbounded operators:

Theorem 1. *For the evolution described in Eq. (1), derivative of the QFI of evolving state $\rho(t,\varphi)$ over time is fundamentally bounded by*

$$\frac{dI_\varphi(t)}{dt} \leq 4 \min_h \left(\langle \mathfrak{a}(h) \rangle + \sqrt{\langle \mathfrak{b}(h)^2 \rangle \, I_\varphi(t)} \right), \tag{B1}$$

where the optimization variable

$$h = \left(\begin{array}{c|c} h_{00} & \vec{h}^\dagger \\ \hline \vec{h} & \mathfrak{h} \end{array} \right) \tag{B2}$$

is an $(J+1)\times(J+1)$ Hermitian matrix with a block structure, where $\mathfrak{h} \in \mathbb{C}_H^{J\times J}$ is an $J \times J$ hermitian matrix, $\vec{h} \in \mathbb{C}^J$ is a complex vector of length J, $h_{00} \in \mathbb{R}$, $\langle\cdot\rangle$ is an expectation value, while $\mathfrak{a}(h)$, $\mathfrak{b}(h)$ are operators defined as:

$$\begin{aligned} \mathfrak{a}(h) &= \left(i\dot{\vec{L}} + \mathfrak{h}\vec{L} + \vec{h}\mathbb{1} \right)^\dagger \left(i\dot{\vec{L}} + \mathfrak{h}\vec{L} + \vec{h}\mathbb{1} \right), \\ \mathfrak{b}(h) &= \dot{H} - \frac{i}{2}\left(\dot{\vec{L}}^\dagger \vec{L} - \vec{L}^\dagger \dot{\vec{L}} \right) + h_{00}\mathbb{1} + \vec{L}^\dagger \vec{h} + \vec{h}^\dagger \vec{L} + \vec{L}^\dagger \mathfrak{h} \vec{L}. \end{aligned} \tag{B3}$$

Here $\dot{X} = \partial_\varphi X$ denotes derivative over parameter, $\vec{L} = [L_1, ..., L_J]^T$ is a vector of Linblad operators.

A similar (and slightly stronger) bound has been derived with alternative methods in [20]. To prove Eq. (B1), we start we the stronger version of the results from [16], generalized for unbounded operators:

Lemma 2. *Consider the state ρ_φ depending on the unknown parameter φ, which is next treated as an input for the channel depended on the same parameter $\Lambda_\varphi[\cdot] = \sum_{k=0}^J K_k(\varphi) \cdot K_k^\dagger(\varphi)$. Then the difference between QFI of the the final state $\Lambda_\varphi[\rho_\varphi]$ and ρ_φ is bounded by:*

$$I_\varphi[\Lambda_\varphi[\rho_\varphi]] - I_\varphi[\rho_\varphi] \leq 4 \left(\langle \alpha \rangle + \sqrt{\langle \beta^2 \rangle \, I_\varphi[\rho_\varphi]} \right) \tag{B4}$$

where $\alpha = \dot{\vec{K}}^\dagger \dot{\vec{K}}$, $\beta = i\vec{K}^\dagger \dot{\vec{K}}$.

Proof. See [72].□

Having that, we can prove Theorem 1.

Proof of Theorem 1. The evolution govern by Lindblad equation for small time Δt may be approximated up to terms $\mathcal{O}(\Delta t^{3/2})$ by acting the Kraus operators [19]:

$$K_0 = \mathbb{1} - \left(iH + \frac{1}{2}\vec{L}^\dagger \vec{L} \right) \Delta t + \mathcal{O}(\Delta t^{3/2}), \tag{B5}$$

$$\vec{K} = \vec{L}\sqrt{\Delta t} + \mathcal{O}(\Delta t). \tag{B6}$$

After substituting to Eq. (B4), deviding both sides by Δt and taking limit $\Delta t \to 0$ one obtains:

$$\frac{dI_\varphi(t)}{dt} \leq 4 \left(\langle \mathfrak{a} \rangle + \sqrt{\langle \mathfrak{b}^2 \rangle \, I_\varphi(t)} \right), \tag{B7}$$

where $\mathfrak{a} = \dot{\vec{L}}^\dagger \dot{\vec{L}}$, $\mathfrak{b} = \dot{H} - \frac{i}{2}(\dot{\vec{L}}^\dagger \vec{L} - \vec{L}^\dagger \dot{\vec{L}})$.

Next, note, that both Kraus representation and Lindblad representation are not unique. To make the bound tighter, in [17, 19] optimization over Kraus representation has been performed. Here we perform analogical optimization over the Lindblad operator, leading to the same result. Indeed, after substitution:

$$\begin{aligned} \vec{L}' &= e^{-i\mathfrak{h}\varphi}\vec{L} + \varphi\vec{h}\mathbb{1}, \\ H' &= H + \frac{\varphi}{2i}\left[\vec{h}^\dagger \vec{L} - \vec{L}^\dagger \vec{h} \right] + \varphi h_{00}\mathbb{1}, \end{aligned} \tag{B8}$$

the evolution remains unchanged, so one may optimize the bound Eq. (B7) over h to get Eq. (B1).

Appendix C: Calculations of bound for discussed examples

Frequency estimation. For frequency estimation Sec. III A for making $\mathfrak{b}(h) = 0$, only the diagonal elements of h are important. Setting all off-diagonal elements equal to 0 we have:

$$\begin{aligned} \mathfrak{b}(h) &= a^\dagger a + h_{00} + h_{11}\Gamma(1+n_E)a^\dagger a + h_{22}\Gamma n_E a a^\dagger, \\ \mathfrak{a}(h) &= (h_{11})^2\Gamma(1+n_E)a^\dagger a + (h_{22})^2\Gamma n_E a a^\dagger, \end{aligned} \tag{C1}$$

so the problem is formulated as:

$$\min_{h_{00},h_{11},h_{22}} (h_{11})^2\Gamma(1+n_E)\langle a^\dagger a\rangle + (h_{22})^2\Gamma n_E(\langle a^\dagger a\rangle + 1), \quad \text{with} \quad \begin{cases} 1 + h_{11}\Gamma(1+n_E) + h_{22}\Gamma n_E = 0, \\ h_{00} + h_{22}\Gamma n_E = 0, \end{cases} \tag{C2}$$

which after direct optimization gives:

$$\langle \mathfrak{a}(h) \rangle = \frac{\langle a^\dagger a\rangle}{\Gamma(1+2n_E - \frac{n_E}{\langle a^\dagger a\rangle + 1})} \overset{\langle a^\dagger a\rangle \gg 1}{\approx} \frac{\langle a^\dagger a\rangle}{\Gamma(1+2n_E)}. \tag{C3}$$

Displacement estimation. For displacement estimation Sec. III B, for making $\mathfrak{b}(h) = 0$, only the $\vec{h}$ elements of h are important:

$$\begin{aligned} \mathfrak{b}(h) =& ia^\dagger - ia + h_{01}\sqrt{\Gamma(1+n_E)}a + h_{02}\sqrt{\Gamma n_E}a^\dagger, \\ &+ h_{10}\sqrt{\Gamma(1+n_E)}a^\dagger + h_{20}\sqrt{\Gamma n_E}a \\ \mathfrak{a}(h) =& (|h_{01}|^2 + |h_{02}|^2)\mathbb{1}, \end{aligned} \tag{C4}$$

so:

$$\min_{h_{01},h_{02}} |h_{01}|^2 + |h_{02}|^2, \quad \text{with} \quad \begin{cases} i + h_{01}^*\sqrt{\Gamma(1+n_E)} + h_{02}\sqrt{\Gamma n_E} = 0, \\ -i + h_{01}\sqrt{\Gamma(1+n_E)} + h_{02}^*\sqrt{\Gamma n_E} = 0, \end{cases} \tag{C5}$$

which gives

$$\langle \mathfrak{a}(h) \rangle = \frac{1}{\Gamma(1+2n_E)}. \tag{C6}$$

Squeezing estimation. For squeezing estimation Sec. III C, only off-diagonal element oh $\mathfrak{h}$ are important:

$$\begin{aligned}\mathfrak{b}(h) =& a^2 + a^{\dagger 2} + h_{21} a^2 \Gamma \sqrt{n_E(1+n_E)} \\ &+ h_{12} a^{\dagger 2} \Gamma \sqrt{n_E(1+n_E)} \\ \mathfrak{a}(h) =& |h_{12}|^2 (2a^\dagger a + 1)\Gamma\sqrt{n_E(1+n_E)}.\end{aligned} \tag{C7}$$

The unique solution giving $\mathfrak{b}(h) = 0$ is therefore $h_{12} = -(\Gamma\sqrt{n_E(1+n_E)})^{-1}$, which gives:

$$\langle \mathfrak{a}(h) \rangle = \frac{2\langle a^\dagger a\rangle + 1}{\Gamma\sqrt{n_E(1+n_E)}}. \tag{C8}$$

Appendix D: Squeezing estimation – QEC

Assume that the states of the system $\mathcal{H}_S$ may be entangled with a noiseless ancilla $\mathcal{H}_A$. An effective quantum error correction protocol for estimating Hamiltonian H may be applied iff there exists a proper code space $\mathcal{H}_C \subset \mathcal{H}_S \otimes \mathcal{H}_A$ satisfying (for simplicity we consider the situation when there is only one Linbdlad operator, which is our case)[17]:

$$\begin{aligned}&\Pi_C(\dot{H} \otimes \mathbb{1}_A)\Pi_C \not\propto \mathbb{1} \\ &\Pi_C(L \otimes \mathbb{1}_A)\Pi_C = \lambda \mathbb{1} \\ &\Pi_C(L^\dagger L \otimes \mathbb{1}_A)\Pi_C = \mu \mathbb{1},\end{aligned} \tag{D1}$$

where Π_C is a projection onto code space $\mathcal{H}_C$, $\dot{H}$ denotes the derivative of Hamiltonian over the estimated parameter, while λ and μ are scalars. Once the above are satisfied, after applying a proper QEC, one obtains a unitary evolution $U = \exp(-it\Pi_C(H \otimes \mathbb{1}_A)\Pi_C)$ on this subspace.

The first condition guarantees, that the Hamiltonian acts non-trivially inside of the code space, so there appears the signal to be measured. The second condition guarantees, that the noise does not act inside of the code space (it may only take the state outside of it). The last condition is induced to guarantee, that the orthogonal states of the code space are still perfectly distinguishable after acting the noise, which is necessary for performing QEC.

To satisfy conditions Eq. (D1) in squeezing estimation problem Sec. III C we choose the subspace spanned by two states:

$$\begin{aligned}|c_0\rangle &= \tfrac{1}{\sqrt{2}}(|N-2\rangle + |N\rangle) \otimes |0\rangle_A \\ |c_1\rangle &= \tfrac{1}{\sqrt{2}}(|N-2\rangle - |N\rangle) \otimes |1\rangle_A,\end{aligned} \tag{D2}$$

where $|0\rangle_A, |1\rangle_A$ are mutually orthogonal states of ancilla.

One can easily check that $\Pi_C(\dot{H} \otimes \mathbb{1}_A)\Pi_C = \sqrt{N(N-2)}\sigma_z$, which would lead to $F = 4N(N-2)t^2$.

Appendix E: Squeezing estimation – cat state protocol

Here we will argue, that for small time satisfying $t\epsilon \ll 1/\sqrt{N+2}$, acting of Hamiltonian $\epsilon(a^{\dagger 2} + a^2)$ on cat states may be well approximated by:

$$\begin{aligned}(a^{\dagger 2} + a^2)\,|\mathcal{C}^\pm_\alpha\rangle &\approx 2\mathrm{Re}(\alpha^2)\,|\mathcal{C}^\pm_\alpha\rangle, \\ (a^{\dagger 2} + a^2)\,|\mathcal{C}^\pm_{i\alpha}\rangle &\approx -2\mathrm{Re}(\alpha^2)\,|\mathcal{C}^\pm_\alpha\rangle.\end{aligned} \tag{E1}$$

I.e., the correction to this approximation, even accumulated over this time, is still negligible.

First, answer simpler questions. Trivially $a\,|\alpha\rangle = \alpha\,|\alpha\rangle$. But how $a^\dagger\,|\alpha\rangle$ is close to $\alpha^*\,|\alpha\rangle$? Projection of $a^\dagger\,|\alpha\rangle$ on $|\alpha\rangle$ gives:

$$|\,\langle\alpha|a^\dagger|\alpha\rangle\,|^2 = |\alpha|^2 \tag{E2}$$

while the norm of $a^\dagger\,|\alpha\rangle$ is

$$|\,\langle\alpha|aa^\dagger|\alpha\rangle\,|^2 = |\alpha|^2 + 1, \tag{E3}$$

from which:

$$a^\dagger\,|\alpha\rangle = \alpha^*\,|\alpha\rangle + |\alpha^\perp\rangle \tag{E4}$$

where $|\alpha^\perp\rangle$ is normalized an orthogonal to α

Similar reasoning may be performed for $a^{\dagger 2}\,|\alpha\rangle$ and $\alpha^{*2}\,|\alpha\rangle$. The protection of $a^{\dagger 2}\,|\alpha\rangle$ on $|\alpha\rangle$ gives:

$$|\,\langle\alpha|a^{\dagger 2}|\alpha\rangle\,|^2 = |\alpha|^4 \tag{E5}$$

while the norm of $a^{\dagger 2}\,|\alpha\rangle$ is:

$$|\,\langle\alpha|a^2a^{\dagger 2}|\alpha\rangle\,|^2 = |\alpha|^4 + 4|\alpha|^2 + 2 \tag{E6}$$

so

$$(a^\dagger)^2\,|\alpha\rangle = (\alpha^*)^2\,|\alpha\rangle + \sqrt{4|\alpha|^2+2}\,|\alpha'^\perp\rangle \tag{E7}$$

Therefore we have:

$$\begin{aligned}\|(a^{\dagger 2} + a^2)\,|\mathcal{C}^\pm_\alpha\rangle - 2\mathrm{Re}(\alpha^2)\,|\mathcal{C}^\pm_\alpha\rangle\,\| &= \sqrt{4|\alpha|^2+2}, \\ \|(a^{\dagger 2} + a^2)\,|\mathcal{C}^\pm_{i\alpha}\rangle - 2\mathrm{Re}(\alpha^2)\,|\mathcal{C}^\pm_\alpha\rangle\,\| &= \sqrt{4|\alpha|^2+2}.\end{aligned} \tag{E8}$$

Now let us look, at how the correction may accumulate over time. We start from state $|\psi(0)\rangle$ and analyze its evolution govern by Hamiltonian H, namely $|\psi(t)\rangle = e^{-itH}\,|\psi(0)\rangle$. Let H_C be an approximation of H. The question is: how well Hamiltonian H may be approximated by H_C? More precisely, having $|\psi_C(t)\rangle = e^{-itH_C}\,|\psi(0)\rangle$, what will be the bound for $\|\,|\psi(t)\rangle - |\psi_C(t)\rangle\,\|$? By direct calculation:

$$\begin{aligned}&\frac{d}{dt}\left[(\langle\psi(t)| - \langle\psi_C(t)|)(|\psi(t)\rangle - |\psi_C(t)\rangle)\right] = \\ &2\mathrm{Im}\,\langle\psi(t)|(H - H_C)|\psi_C(t)\rangle \le 2\|(H-H_C)\,|\psi_C(t)\rangle\,\|,\end{aligned} \tag{E9}$$

so

$$\|\,|\psi(t)\rangle - |\psi_C(t)\rangle\,\|^2 \le 2t \max_{t'\in[0,t]} \|(H-H_C)\,|\psi_C(t')\rangle\,\|. \tag{E10}$$

In our case:

$$\max_{t'\in[0,t]} \|(H-H_C)\,|\psi_C(t')\rangle\,\| \le \epsilon\sqrt{4|\alpha|^2+2}, \tag{E11}$$

so

$$\|\,|\psi(t)\rangle - |\psi_C(t)\rangle\,\| \le t\epsilon\sqrt{4N+2}, \tag{E12}$$

Appendix F: Loss rate estimation

Here we derive the formula for classical FI with respect to Γ for the parity counting measurement, applying for squeezed vacuum state after short evolution $(N+1)\Gamma t(n_E+1) \ll 1$. Especially, we clarified, why it contains as much information as exact photon counting.

First note that as the classical FI information is equal

$$F_\Gamma = \sum_i p(i) \left(\frac{\partial_\varphi p(i)}{p(i)} \right)^2, \tag{F1}$$

two measurement results i, j may be merged without loss if $(\partial_\Gamma p(i)/p(i))^2 = (\partial_\Gamma p(j)/p(j))^2$. Second, for two-outcomes measurement $p(0) = 1-\epsilon\varphi$, $p(1) = \epsilon\varphi$, the part $p(0)(\partial_\varphi p(0)/p(0))^2 \approx \epsilon^2$ is negligible comparing to $p(1)(\partial_\varphi p(1)/p(1))^2 \approx \epsilon/\varphi$ for small $\epsilon\varphi$. Having this we are ready to analyze photon losses.

First, consider the Fock input state for simplicity:

$$p(n) = 1 - tn\Gamma(1+n_E) - t(n+1)\Gamma n_E \tag{F2}$$
$$p(n+1) = t(n+1)\Gamma n_E \tag{F3}$$
$$p(n-1) = tn\Gamma(1+n_E). \tag{F4}$$

Then indeed the results $p(n-1), p(n+1)$ contain the majority of information, and they may be merged without loss, as

$$\left(\frac{\partial_\Gamma p(n-1)}{p(n-1)} \right)^2 = \left(\frac{\partial_\Gamma p(n+1)}{p(n+1)} \right)^2 = \frac{1}{\Gamma}, \tag{F5}$$

so FI is

$$F_\Gamma \approx \frac{p(n-1)+p(n+1)}{\Gamma} = \frac{n(1+2n_E)+n_E}{\Gamma}. \tag{F6}$$

Next, note that for the squeezed vacuum input state, for any odd n the ratio $(\partial_\Gamma p(n)/p(n))^2$ will still be equal to $1/\Gamma$. The total probability of getting an odd number of photons will be the sum of the probability of losing one photon and taking one photon from the environment, which are given as:

$$\begin{aligned} p_{\text{losing}} &= \sum_n p_{\text{in}}(n) n\Gamma t(1+n_E) \\ p_{\text{taking}} &= \sum_n p_{\text{in}}(n)(n+1)\Gamma t n_E \end{aligned} \tag{F7}$$

so finally $p_{\text{odd}} = \Gamma t[N(2n_E+1)+n_E]$ and $F_\Gamma \approx t[N(2n_E+1)+n_E]/\Gamma$.

One can note that for very large k probability of obtaining $p(2k+1)$ cannot be approximating by the first order as $p(2k+1) \approx t(2k+1)\Gamma(1+n_E)p_{\text{in}}(2k) + t(2k+2)\Gamma n_E p_{\text{in}}(2k+2)$, since condition $(k+1)\Gamma t(n_E+1) \ll 1$ will not be satisfied. Anyway, its impact will be negligible, as $p_{\text{in}}(2k)$ decreases exponentially with increasing k.

Appendix G: Temperature estimation

Here we discuss the example of temperature estimation, comparing the results to the bounds existing in the literature and investigating details of exemplary optimal strategy based on the usage of Fock states.

First, recall the bound from [50, 58], derived for the passive strategy, i.e. one prepare input state, let it evolve for time t without any additional actions, and perform a measurement. Eq. (9) with $H = 0$, after interrogation over time t, may be seen as mixing mode a with thermal mode b via beamsplitter with transitivity $\kappa = e^{-t\Gamma}$, i.e.:

$$\begin{aligned} \hat{a}' &= \sqrt{\kappa}\hat{a} + \sqrt{1-\kappa}\hat{b}, \\ \hat{b}' &= -\sqrt{1-\kappa}\hat{a} + \sqrt{\kappa}\hat{b}. \end{aligned} \tag{G1}$$

For such a formulated problem, the QFI of the output state may be bounded using the method based on channel purification, which gives [50, 58][2]:

$$I_{n_E} \leq \frac{1}{n_E(n_E + \frac{1}{1-\kappa})} + \frac{\kappa N(2n_E+1)(1-\kappa)}{n_E(n_E+1)(n_E(1-\kappa)+1)^2}. \tag{G2}$$

By direct calculation, one can see that in the limit of short times, $(1+n_E)t\Gamma \ll 1$ it converges to Eq. (33).

Technical details of computation of FI for Fock state. Starting with twin-Fock state $|m,n\rangle$, probability of obtaining twin-Fock state $|m',n'\rangle$ after going through beam splitter with transitivity κ is given as [73]:

$$p(n',m'|n,m) = \frac{n'!m'!}{n!m!} \left[\sum_{i=0}^{n} \sum_{j=0}^{m} \binom{n}{i} \binom{m}{j} \right.$$
$$\left. (-1)^j \sqrt{\kappa}^{n+m-i-j} \sqrt{1-\kappa}^{i+j} \delta_{n-i+j,n'} \delta_{m-j+i,m'} \right]^2, \tag{G3}$$

where two last deltas imply, that non-zero value may be obtained only for $n'+m' = n+m$. For shorter notation, we define therefore:

$$p(n'|n,m) = \begin{cases} p(n', n+m-n'|n,m), & \text{if } n'-n \leq m \\ 0, & \text{otherwise.} \end{cases} \tag{G4}$$

As the thermal state is a mixture (not superposition) of the Fock state with $p_{n_B}(m) = \frac{n_B^m}{(n_B+1)^{m+1}}$, by tracing out the environment we have:

$$p(n'|n) = \sum_{m=0}^{\infty} p_{n_B}(m) p(n'|n,m). \tag{G5}$$

Clasical FI is equal $\sum_{n'=0}^{\infty} (\partial_{n_E} p(n'|n))^2 / p(n'|n)$. Note, that n_E dependence lies only in $p_{n_E}(m)$, and therefore:

$$F_{n_E} = \sum_{n'=0}^{\infty} \frac{(\sum_{m=0}^{\infty} [\partial_{n_E} p_{n_E}(m)] p(n'|n,m))^2}{\sum_{m=0}^{\infty} p_{n_B}(m) p(n'|n,m)}. \tag{G6}$$

For low temperatures, the sums converge rather quickly, so they may be effectively computed by introducing a numerical cutoff.

[2] Note that in [50] some typos appear in the finite formula in App. A. Correct result may be obtained by substituting Eqs. (4), (5) to Eq. (A4). In [58] the formula concerns another parameter $n_B = (1-\kappa)n_E$, so $F_{n_E} = F_{n_B}(1-\kappa)^2$

Appendix H: Random displacement with Gaussian distribution vs. temperature estimation

Here we discuss the relation between random displacement with Gaussian distribution and temperature estimation. Let us come back to the problem of displacement estimation, but assume that neither intensity more direction of displacement α is fixed, but α is a random complex Gaussian variable with zero mean $p(\alpha) = \frac{1}{\pi\sigma^2}\exp(-|\alpha|^2/\sigma^2)$ and the aim is to estimate the variance of these distribution σ^2. For a fixed time (i.e. time dependence was not taken into account), such a problem has been discussed in [58] in the context of dark matter sensing. Let us recall the crucial observations.

Consider the quantum channel consisting displacement β and mixing with thermal mode b_{n_E} (where n_E is mean number of thermal photons):

$$a' = \sqrt{\kappa}a + \beta + \sqrt{1-\kappa}b_{n_E}. \tag{H1}$$

If β is a random complex variable with Gaussian distribution $p(\beta) = \frac{1}{\pi\sigma^2}\exp(-|\beta|^2/\sigma^2)$, this channel is exactly equivalent to solely mixing with thermal mode with properly more thermal photons:

$$a' = \sqrt{\kappa}a + \sqrt{1-\kappa}b_{n_E+n_\beta}, \quad \text{where} \quad n_\beta = \frac{\sigma^2}{1-\kappa} \tag{H2}$$

Now we are ready to consider time dependence. Eq. (9) with Hamiltonian Eq. (15), for any fixed α leads to the mode transformation:

$$a' = e^{-t\Gamma/2}a + 2\alpha(1-e^{-t\Gamma/2})/(\Gamma/2) + \sqrt{1-e^{-t\Gamma}}b_{n_E}. \tag{H3}$$

If α is a random complex variable with distribution $p(\alpha) = \frac{1}{\pi\sigma^2}\exp(-|\alpha|^2/\sigma^2)$, this is equivalent to:

$$a' = e^{-t\Gamma/2}a + \sqrt{1-e^{-t\Gamma}}b_{n_E+n_\alpha(t)} \tag{H4}$$

where:

$$n_\alpha(t) = \frac{\sigma^2\left[2\alpha(1-e^{-t\Gamma/2})/(\Gamma/2)\right]^2}{1-e^{-t\Gamma}}. \tag{H5}$$

We see that for any fixed time, we may map the channel obtained in this way for the channel solely mixing with a thermal bath. However, the effective number of thermal photons $n_E + n_A(t)$ is a function of time, therefore conclusions about optimal time-dependent strategy will be substantially different. Especially, for short times $n_\alpha(t)$ arises quadratically with t, so, unlike in temperature estimation, the fast-prepare-and-measure protocol will be far from being optimal.

We should stress that in the above calculation, the perfect coherence in time of the variable α is assumed (i.e. once it is randomly drawn from Gaussian distribution, it remains fixed for any time). In the context of dark matter sensing, also changes of α in time should be included. See [62] for a realistic approach to time-dependence in this problem.

[1] V. Giovannetti, S. Lloyd, and L. Maccone, Quantum metrology, Phys. Rev. Lett. **96**, 010401 (2006).
[2] M. G. A. Paris, Quantum estimation for quantum technologies, Int. J. Quantum Inf. **07**, 125 (2009).
[3] V. Giovannetti, S. Lloyd, and L. Maccone, Advances in quantum metrology, Nat. Photonics **5**, 222 (2011).
[4] G. Toth and I. Apellaniz, Quantum metrology from a quantum information science perspective, J. Phys. A: Math. Theor. **47**, 424006 (2014).
[5] R. Demkowicz-Dobrzański, M. Jarzyna, and J. Kołodyński, Chapter four - quantum limits in optical interferometry (Elsevier, 2015) pp. 345–435.
[6] R. Schnabel, Squeezed states of light and their applications in laser interferometers, Phys. Rep. **684**, 1 (2017).
[7] C. L. Degen, F. Reinhard, and P. Cappellaro, Quantum sensing, Rev. Mod. Phys. **89**, 035002 (2017).
[8] L. Pezzè, A. Smerzi, M. K. Oberthaler, R. Schmied, and P. Treutlein, Quantum metrology with nonclassical states of atomic ensembles, Rev. Mod. Phys. **90**, 035005 (2018).
[9] S. Pirandola, B. R. Bardhan, T. Gehring, C. Weedbrook, and S. Lloyd, Advances in photonic quantum sensing, Nat. Photonics **12**, 724 (2018).
[10] A. Fujiwara and H. Imai, A fibre bundle over manifolds of quantum channels and its application to quantum statistics, J. Phys. A: Math. Theor. **41**, 255304 (2008).
[11] B. Escher, R. de Matos Filho, and L. Davidovich, General framework for estimating the ultimate precision limit in noisy quantum-enhanced metrology, Nat. Phys. **7**, 406 (2011).
[12] R. Demkowicz-Dobrzański, J. Kołodyński, and M. Guţă, The elusive heisenberg limit in quantum-enhanced metrology, Nat. Commun. **3**, 1063 (2012).
[13] S. I. Knysh, E. H. Chen, and G. A. Durkin, True limits to precision via unique quantum probe, arXiv:1402.0495 (2014).
[14] R. Demkowicz-Dobrzański and L. Maccone, Using entanglement against noise in quantum metrology, Phys. Rev. Lett. **113**, 250801 (2014).
[15] S. Zhou and L. Jiang, Asymptotic theory of quantum channel estimation, PRX Quantum **2**, 010343 (2021).
[16] S. Kurdziałek, W. Górecki, F. Albarelli, and R. Demkowicz-Dobrzański, Using adaptiveness and causal superpositions against noise in quantum metrology, Phys. Rev. Lett. **131**, 090801 (2023).
[17] S. Zhou, M. Zhang, J. Preskill, and L. Jiang, Achieving the heisenberg limit in quantum metrology using quantum error correction, Nat. Commun. **9**, 78 (2018).
[18] A. Das, W. Gorecki, and R. Demkowicz-Dobrzanski, Universal time scalings of sensitivity in markovian quantum metrology, arXiv preprint arXiv:2404.03954 10.48550/arXiv.2404.03954 (2024).
[19] R. Demkowicz-Dobrzański, J. Czajkowski, and P. Sekatski, Adaptive quantum metrology under general markovian noise, Phys. Rev. X **7**, 041009 (2017).
[20] K. Wan and R. Lasenby, Bounds on adaptive quantum metrology under markovian noise, Phys. Rev. Res. **4**, 033092 (2022).
[21] V. Giovannetti and L. Maccone, Sub-heisenberg estimation strategies are ineffective, Phys. Rev. Lett. **108**, 210404 (2012).

[22] H. I. Nurdin and M. Guţă, Parameter estimation and system identification for continuously-observed quantum systems, Annual Reviews in Control , S1367578822000268 (2022), arXiv:2205.11977.

[23] M. A. C. Rossi, F. Albarelli, D. Tamascelli, and M. G. Genoni, Noisy Quantum Metrology Enhanced by Continuous Nondemolition Measurement, Phys. Rev. Lett. **125**, 200505 (2020), arXiv:2006.08974.

[24] J. Amorós-Binefa and J. Kołodyński, Noisy atomic magnetometry in real time, New J. Phys. **23**, 123030 (2021), arXiv:2103.12025.

[25] J. Boeyens, B. Annby-Andersson, P. Bakhshinezhad, G. Haack, M. Perarnau-Llobet, S. Nimmrichter, P. P. Potts, and M. Mehboudi, Probe thermometry with continuous measurements, New J. Phys. **25**, 123009 (2023), arXiv:2307.13407.

[26] L. Garbe, M. Bina, A. Keller, M. G. A. Paris, and S. Felicetti, Critical quantum metrology with a finite-component quantum phase transition, Phys. Rev. Lett. **124**, 120504 (2020).

[27] M.-L. Cai, Z.-D. Liu, W.-D. Zhao, Y.-K. Wu, Q.-X. Mei, Y. Jiang, L. He, X. Zhang, Z.-C. Zhou, and L.-M. Duan, Observation of a quantum phase transition in the quantum Rabi model with a single trapped ion, Nat. Commun. **12**, 1126 (2021).

[28] L. Garbe, O. Abah, S. Felicetti, and R. Puebla, Critical quantum metrology with fully-connected models: from heisenberg to kibble–zurek scaling, Quantum Science and Technology **7**, 035010 (2022).

[29] K. Gietka, L. Ruks, and T. Busch, Understanding and improving critical metrology. quenching superradiant light-matter systems beyond the critical point, Quantum **6**, 700 (2022).

[30] R. Di Candia, F. Minganti, K. V. Petrovnin, G. S. Paraoanu, and S. Felicetti, Critical parametric quantum sensing, npj Quantum Inf. **9**, 23 (2023).

[31] U. Alushi, W. Górecki, S. Felicetti, and R. Di Candia, Optimality and Noise Resilience of Critical Quantum Sensing, Phys. Rev. Lett. **133**, 040801 (2024).

[32] A. Cabot, F. Carollo, and I. Lesanovsky, Continuous sensing and parameter estimation with the boundary time crystal, Phys. Rev. Lett. **132**, 050801 (2024).

[33] U. Alushi, A. Coppo, V. Brosco, R. Di Candia, and S. Felicetti, Collective quantum enhancement in critical quantum sensing, arXiv preprint arXiv:2407.18055 (2024).

[34] T. Ilias, D. Yang, S. F. Huelga, and M. B. Plenio, Criticality-Enhanced Quantum Sensing via Continuous Measurement, PRX Quantum **3**, 010354 (2022), arXiv:2108.06349.

[35] R. Salvia, M. Mehboudi, and M. Perarnau-Llobet, Critical Quantum Metrology Assisted by Real-Time Feedback Control, Phys. Rev. Lett. **130**, 240803 (2023), arXiv:2211.07688.

[36] A. Cabot, F. Carollo, and I. Lesanovsky, Continuous Sensing and Parameter Estimation with the Boundary Time Crystal, Phys. Rev. Lett. **132**, 050801 (2024), arXiv:2307.13277.

[37] R. Demkowicz-Dobrzański and L. Maccone, Using entanglement against noise in quantum metrology, Phys. Rev. Lett. **113**, 250801 (2014).

[38] L. Ostermann and K. Gietka, Temperature-enhanced critical quantum metrology, Phys. Rev. A **109**, L050601 (2024).

[39] L. A. Souza, Classes of gaussian states for squeezing estimation, Physics Letters A , 129431 (2024).

[40] V. Giovannetti, S. Lloyd, and L. Maccone, Quantum measurement bounds beyond the uncertainty relations, Phys. Rev. Lett. **108**, 260405 (2012).

[41] M. J. W. Hall, D. W. Berry, M. Zwierz, and H. M. Wiseman, Universality of the heisenberg limit for estimates of random phase shifts, Phys. Rev. A **85**, 041802 (2012).

[42] W. Górecki, R. Demkowicz-Dobrzański, H. M. Wiseman, and D. W. Berry, π-corrected heisenberg limit, Phys. Rev. Lett. **124**, 030501 (2020).

[43] J. Dalibard, Y. Castin, and K. Mølmer, Wave-function approach to dissipative processes in quantum optics, Phys. Rev. Lett. **68**, 580 (1992).

[44] P. T. Cochrane, G. J. Milburn, and W. J. Munro, Macroscopically distinct quantum-superposition states as a bosonic code for amplitude damping, Phys. Rev. A **59**, 2631 (1999).

[45] Z. Leghtas, G. Kirchmair, B. Vlastakis, R. J. Schoelkopf, M. H. Devoret, and M. Mirrahimi, Hardware-efficient autonomous quantum memory protection, Phys. Rev. Lett. **111**, 120501 (2013).

[46] P. M. Birchall, E. J. Allen, T. M. Stace, J. L. O'Brien, J. C. F. Matthews, and H. Cable, Quantum optical metrology of correlated phase and loss, Phys. Rev. Lett. **124**, 140501 (2020).

[47] I. Gianani, F. Albarelli, A. Verna, V. Cimini, R. Demkowicz-Dobrzanski, and M. Barbieri, Kramers–kronig relations and precision limits in quantum phase estimation, Optica **8**, 1642 (2021).

[48] A. Monras and M. G. A. Paris, Optimal quantum estimation of loss in bosonic channels, Phys. Rev. Lett. **98**, 160401 (2007).

[49] G. Adesso, F. Dell'Anno, S. De Siena, F. Illuminati, and L. A. M. Souza, Optimal estimation of losses at the ultimate quantum limit with non-Gaussian states, Phys. Rev. A **79**, 040305(R) (2009), arXiv:0807.3958.

[50] J. Wang, L. Davidovich, and G. S. Agarwal, Quantum sensing of open systems: Estimation of damping constants and temperature, Physical Review Research **2**, 033389 (2020).

[51] R. Jonsson and R. Di Candia, Gaussian quantum estimation of the loss parameter in a thermal environment, Journal of Physics A: Mathematical and Theoretical **55**, 385301 (2022).

[52] C. N. Gagatsos, B. A. Bash, S. Guha, and A. Datta, Bounding the quantum limits of precision for phase estimation with loss and thermal noise, Phys. Rev. A **96**, 062306 (2017).

[53] M. A. C. Rossi, F. Albarelli, and M. G. A. Paris, Enhanced estimation of loss in the presence of kerr nonlinearity, Phys. Rev. A **93**, 053805 (2016).

[54] K. V. Hovhannisyan, M. R. Jørgensen, G. T. Landi, A. M. Alhambra, J. B. Brask, and M. Perarnau-Llobet, Optimal quantum thermometry with coarse-grained measurements, PRX Quantum **2**, 020322 (2021).

[55] P. Sekatski and M. Perarnau-Llobet, Optimal nonequilibrium thermometry in Markovian environments, Quantum **6**, 869 (2022).

[56] A. V. Dixit, S. Chakram, K. He, A. Agrawal, R. K. Naik, D. I. Schuster, and A. Chou, Searching for dark matter with a superconducting qubit, Phys. Rev. Lett. **126**, 141302 (2021).

[57] A. Agrawal, A. V. Dixit, T. Roy, S. Chakram, K. He, R. K. Naik, D. I. Schuster, and A. Chou, Stimulated emission of signal photons from dark matter waves, Phys. Rev. Lett. **132**, 140801 (2024).

[58] H. Shi and Q. Zhuang, Ultimate precision limit of noise sensing and dark matter search, npj Quantum Information **9**, 27 (2023).

[59] S. Pirandola and C. Lupo, Ultimate precision of adaptive noise estimation, Phys. Rev. Lett. **118**, 100502 (2017).

[60] K. Matsumoto, On metric of quantum channel spaces, arXiv preprint arXiv:1006.0300 10.48550/arXiv.1006.0300 (2010).

[61] J. Kolodynski, *Precision bounds in noisy quantum metrology*, Ph.D. thesis, University of Warsaw (2014).

[62] H. Shi, A. J. Brady, W. Górecki, L. Maccone, R. Di Candia, and Q. Zhuang, Quantum-enhanced dark matter detection with in-cavity control: mitigating the rayleigh curse, arXiv preprint arXiv:2409.04656 10.48550/arXiv.2409.04656 (2024).

[63] M. Hayashi, Comparison between the cramer-rao and the mini-

max approaches in quantum channel estimation, Communications in mathematical physics **304**, 689 (2011).

[64] R. Gill and S. Massar, State estimation for large ensembles, Phys. Rev. A **61**, 042312 (2000).

[65] J. Kahn and M. Gutţă, Local asymptotic normality and optimal estimation for d-dimensional quantum systems, in *Quantum stochastics and information: statistics, filtering and control* (World Scientific, 2008) pp. 300–322.

[66] J. Haah, A. W. Harrow, Z. Ji, X. Wu, and N. Yu, Sample-optimal tomography of quantum states, IEEE Transactions on Information Theory **63**, 5628 (2017).

[67] Y. Yang, G. Chiribella, and M. Hayashi, Attaining the ultimate precision limit in quantum state estimation, Communications in Mathematical Physics **368**, 223 (2019).

[68] J. Bavaresco, P. Lipka-Bartosik, P. Sekatski, and M. Mehboudi, Designing optimal protocols in Bayesian quantum parameter estimation with higher-order operations, Phys. Rev. Res. **6**, 023305 (2024).

[69] C. Sánchez Muñoz, G. Frascella, and F. Schlawin, Quantum metrology of two-photon absorption, Phys. Rev. Research **3**, 033250 (2021), arXiv:2105.01561.

[70] S. Panahiyan, C. S. Muñoz, M. V. Chekhova, and F. Schlawin, Two-photon-absorption measurements in the presence of single-photon losses, Phys. Rev. A **106**, 043706 (2022).

[71] A. Karsa, R. Nair, A. Chia, K.-G. Lee, and C. Lee, Optimal quantum metrology of two-photon absorption, Quantum Sci. Technol. **9**, 035042 (2024).

[72] W. Gorecki, M. Hassani, F. Albarelli, and L. Maccone, In preparation.

[73] M. S. Kim, W. Son, V. Bužek, and P. L. Knight, Entanglement by a beam splitter: Nonclassicality as a prerequisite for entanglement, Phys. Rev. A **65**, 032323 (2002).